Collaborative project*

Project acronym: SNM

Project full title: "**Single Nanometer Manufacturing for beyond CMOS devices**"

Grant agreement no: 318804

Deliverable: D11.9 ("Statistical report on scanning probe alignment accuracy")

Name of the coordinating person: Prof. Dr. Ivo W. Rangelow, Email: ivo.rangelow@tu-ilmenau.de

List of participants:

Participant no.	Participant organisation name	Part. short name	Activity Type	Country
1 (Co)	Technische Universität Ilmenau	**TUIL**	HER	Germany
2	EV Group E. Thallner GmbH	**EVG**	IND; End-user	Austria
3	IMEC	**IMEC**	RES	Belgium
4	Mikrosistemi Ltd	**µS**	SME; End-User	Bulgaria
5	Universität Bayreuth	**UBT**	HER	Germany
6	Technische Universiteit Delft	**TUD**	HER	Netherlands
7	Spanish National Research Council	**CSIC**	RES	Spain
8	IBM Research GmbH	**IBM**	IND; End-user	Switzerland
9	École polytechnique fédérale de Lausanne	**EPFL**	HER	Switzerland
10	SwissLitho AG	**SL**	SME; End-User	Switzerland
11	Oxford Instruments Nanotechnology Tools Ltd	**OINT**	IND; End-user	UK
12	Imperial College London	**IMPERIAL**	HER	UK
13	The Open University	**OU**	HER	UK
14	Oxford Scientific Consultants Ltd	**OSC**	SME	UK
15	VSL Dutch Metrology Institute	**VSL**	IND	Netherlands
16	University of Liverpool	**ULIV**	HER	UK

SNM
Work Package 11
Deliverable: D11.9 ("Statistical report on scanning probe alignment accuracy")

Lead beneficiary number	1	**Nature**	R	**Dissemination level**	PU
Estimated Person-months	10				

Person-months by partner for the Deliverable

TUIL							
11,368							

Estimated Delivery Date	M48: 12/2016	**Delivery Date**	23/02/2017
Author	• Valentyn Ishchuk, Ivo W. Rangelow		
Reviewed by:	• WP11 Leader: Thomas Glinsner • WPG4 Leader: Thomas Glinsner • Coordinator: Ivo W. Rangelow		

Criteria and Achieved Results	**Criteria**	**Achieved result**
	Gathering of statistics for measuring the positioning error of the bottom stage carrying the processed semiconductor wafer with respect to the emulated NIL-template chuck.	The established proof-of-concept test bench setup was tested in terms of implemented hard- and software. The setup was used to collect statistical data with regards to the positioning error of the bottom stage carrying the processed wafer. Without temperature compensation an average error of around 10 nm was measured.

Description of the Deliverable	• **Motivation and prerequisites** The downscaling of features sizes of Nanoimprint Lithography (NIL) – patterned structures, defined by the ITRS roadmap (International Technology Roadmap for Semiconductors) [1], is inherently linked with the increasing demand in overlay alignment. For example, sub-10 nm lithography for 9 nm node DRAM requires an overlay accuracy of 1.8 nm 3σ [2, 3], which represents a challenging technological task. The progress in overlay alignment technology indicates that the overlay accuracy achieved with NIL processes is a key factor for low cost mass production of sub-10 nm electronic devices such as NAND Flash memory and DRAM. Template-to-wafer overlay must be ensured on every die. Challenging specifications has to be met, whereas various defects in NIL can be generated from both the template and imprint process [4]. In particular, overlay alignment is a concern for NIL applications using step & repeat techniques (SR-NIL), where successive imprints are repeated in order to pattern large areas [5]. As a consequence, an increased number of high accuracy alignment steps are required. Optical alignment techniques are limited in general by diffraction, which makes alignment accuracies in the sub-10 nm range difficult. The current report presents a new method [6] and a proof-of-concept (PoC) setup for accurately aligning a NIL template with a semiconductor wafer capable for positional accuracy around 10 nm and potentially approaching the 1 nm accuracy. Using the implemented test setup, several measurement studies are addressed in order to evaluate the application of the developed method with respect to the high overlay alignment target. The reported development is based, but not limited to the work described in the following deliverables. - The major requirements and basic specification were developed during the initial project period and is respectively reported in D11.1 (*"Specification protocol for scanning probe alignment step-and-repeat system"*); - The first version of the control electronics was completed and reported in D11.2 (*"SPM multi-channel controller for alignment marks detection"*); - Various algorithms for image recognition and displacement detection were

explored in a simulation environment. The corresponding specification was reported in D11.4 (*"Specification: Algorithms for data recognition, displacement detection, automatic overlay alignment"*);

- First measurement tests of the integrated mini-AFM systems are described in D11.6.
- The system concept was further developed and a software package containing support functions for automatic overlay alignment during a NIL process was designed. The results were presented in D11.7 (*"Data recognition and alignment software"*).
- An automatic control system was developed, described in D11.8.

- **System architecture and components**

Fig. 11.9.1 presents the developed method [6, 7] for accurately aligning a NIL template with a semiconductor wafer capable for positional accuracy preferably better than 10 nm and in particular potentially approaching the 1 nm accuracy. The working principle is described in detail in D11.7. A detailed description of the system architecture of our envisioned NIL tool (see Fig. 11.9.1) and its components is provided in D11.8.

The developed concept of the considered UV-NIL overlay alignment system follows the working principle mentioned above. Herein, the scanning system at the NIL-template is configured to move two mini-AFMs in z-direction, each by using an approach motor. Each single mini-AFM consists of an AFM head and a nanopositioning stage [8]. More details can be found in the deliverable report D11.8.

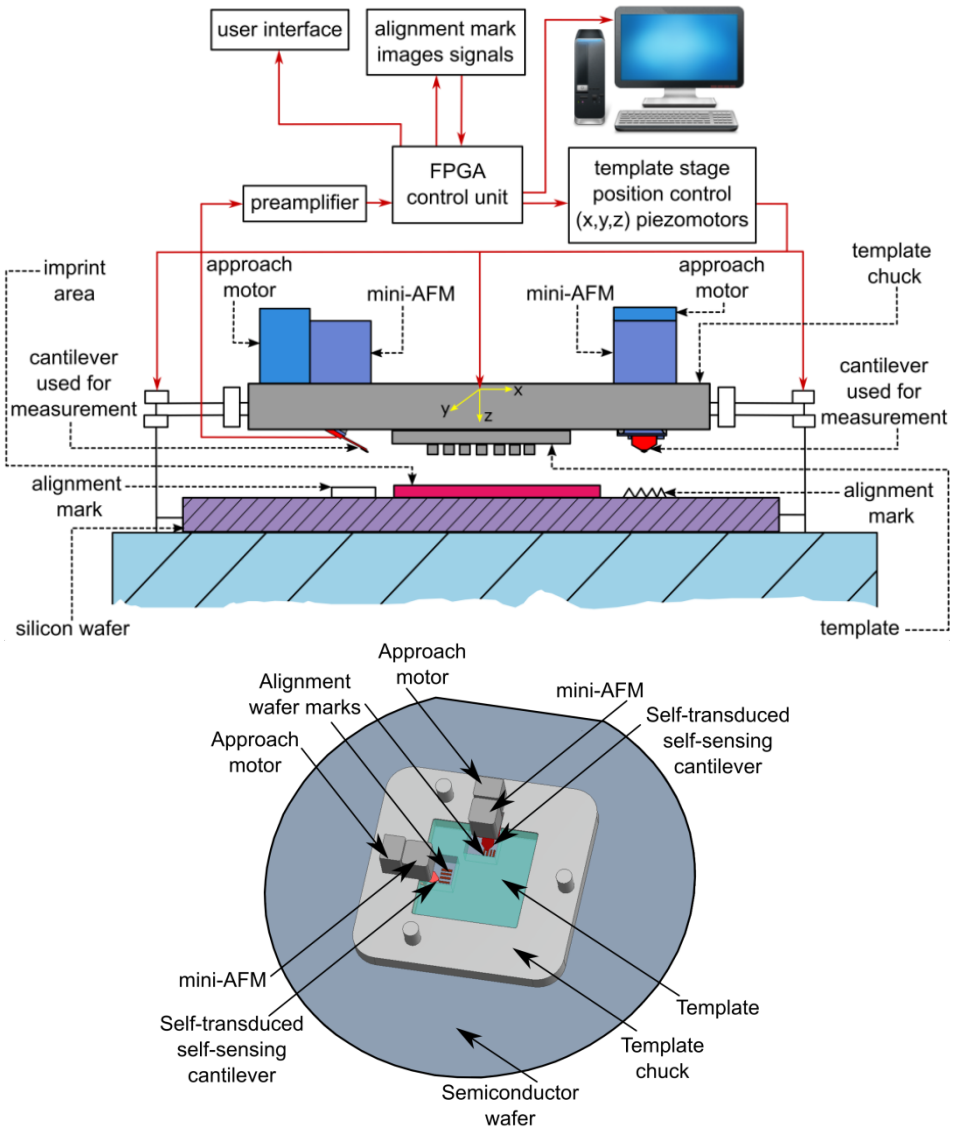

Fig. 11.9.1 Principle of operation of the NIL setup using the developed alignment method. Frontal and top view of the setup [6].

The hardware comprises all key advances that are obligatory for successful high-speed AFM-systems: self-sensing, high-bandwidth self-actuating cantilever, low-noise read-out, high-bandwidth z-control employing direct cantilever actuation, fast top-xy-stage, and a controller for fast data acquisition. The software package is intended to support the automatic overlay alignment during NIL processing. The software consists of two main parts. In particular, the main application includes end-user services such as calibration of the camera-stage system, detection and

alignment of imprint areas as well as a library with supporting functions. A detailed description of the used hardware and software components is given in deliverable report D11.8.

- **Proof of Concept**

The test setup implemented for the developed overlay alignment method is shown in Fig. 11.9.2. The setup is used to emulate the alignment procedure. By using the mini-AFMs of the test bench, alignment marks are detected. As a result the position of the emulated template with respect to the wafer can be estimated. Alignment steps corrects the measured deviation. Further details about the built test bench can be found in the deliverable report D11.6.

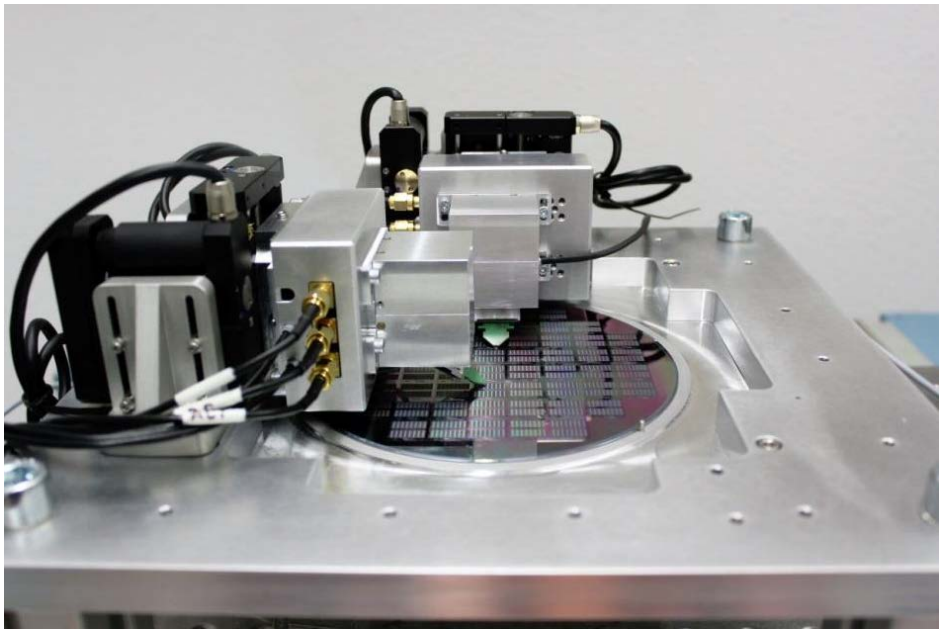

Fig. 11.9.2 Test bench of the alignment proof-of-concept test bench (POC).

For a reliable overlay alignment either the edges or the “center of gravity” of the alignment mark features should be used as input function of the alignment procedure. The “center of gravity” is determined and calculated by the alignment control unit. Within our test the high accuracy detection of the edges of a marker feature was repeated more than 100-times confirming the general principle of operation. As mentioned in the previous periodic report, we used “X”-shaped

alignment marks in order to provide a good features edge contrast for all possible imaging cases. For better pattern detection and recognition a cross-correlation algorithm can be used, like it was shown by Rawlings et al [9]. More information about the reasoning for employing such "X"-marks as well as the description of the alignment mark detection and recognition process (using cross-correlation technique [7, 9]) can be found in deliverable report D11.6.

The used alignment mark pattern is shown in Fig. 11.9.3. It was created by using field-emission scanning probe lithography, followed by a subsequent cryogenic etching step into silicon using SF_6/O_2 plasma [WP1, ref. 10]. It is more convenient to provide a plurality of surface relief markings on the substrate, i.e. alignment features at different locations on the substrate.

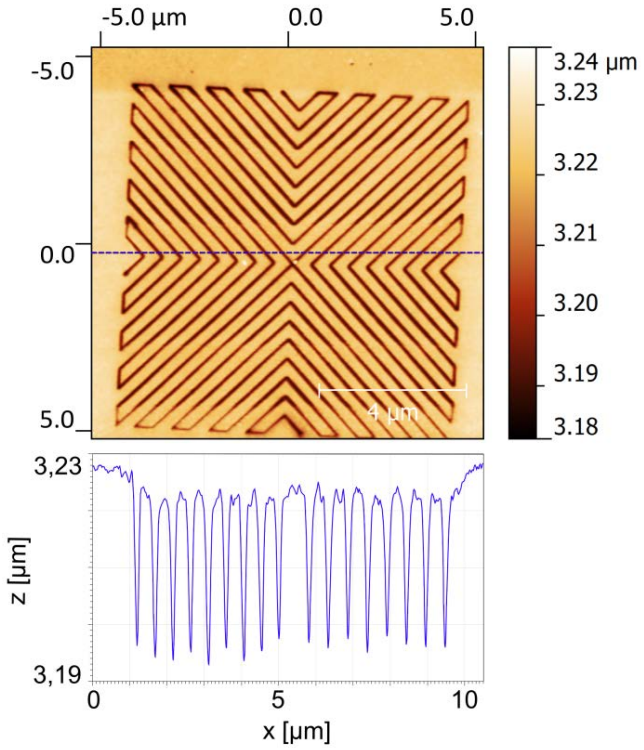

Fig. 11.9.3 AFM image of "X"-shape alignment mark applied during the test procedure. The surface topology profile during AFM-scanning of the utilized "X"-shape alignment mark is shown. The depth of the patterned lines is 30 nm.

Using the topographic information provided by the mini-AFMs the relative position of the alignment mark can be reconstructed. An absolute measurement of the

position of the structure edges is not essentially required. Here, the shape of the signal itself can be used to determine the relative alignment mark position.

As shown in the deliverable report D11.6, the experimental tests confirms that it is feasible to use the patterned alignment mark structure for the alignment procedure even if it is covered with an additional material layer, e.g. with resist. Using the AFM image of the spin-coated sample, the relative position of the alignment mark without resist can be reconstructed.

Once the alignment marks have been patterned and precisely measured, their data can be extracted and applied for different surface coating configurations thus allowing precise alignment of the NIL-Template during the different processing steps of IC manufacturing.

- **Statistical Test results**

In terms of reproducibility tests the topography of a sub-100 nm single trench (see Fig. 11.9.4(a)) was scanned 200-times exclusively in X direction (Y coordinate was kept unchanged) by a single mini-AFM system. Using the obtained multiplicity of scan profiles a standard deviation from the average value was calculated for a single reference point at each of the left and right edge of the trench (see Fig. 11.9.4(b)). The deviation values for trench edges are located within a 3σ of ±3-4 nm.

Such a large deviation in the system can have a significant impact in case of sub-10 nm alignment. There are several reasons for this deviation. First, the value of scan resolution (the size of one pixel in nm) is affecting the value of 3σ directly. In contrast to the actual used scan resolution (256 pixel/line, 500 nm scan area), where the pixel size was 1.9 nm, the pixel size of 0.5 nm (achievable either by enhancement of the scan resolution, e.g. 1024 pixel/line, or by reduction of the scan area) will significantly reduce the measurement deviation. Herein, the actual measurement in Fig. 11.9.4 was limited since our focus was placed on minimization of computational efforts. Taking into account that the PoC system is operated without thermal stabilization, in conjunction with the measurement time, the deviation presented in

Fig. 11.9.4 can be explained. Thus, we suppose that in case of employing the system under cleanroom conditions the deviation value should be further reducible.

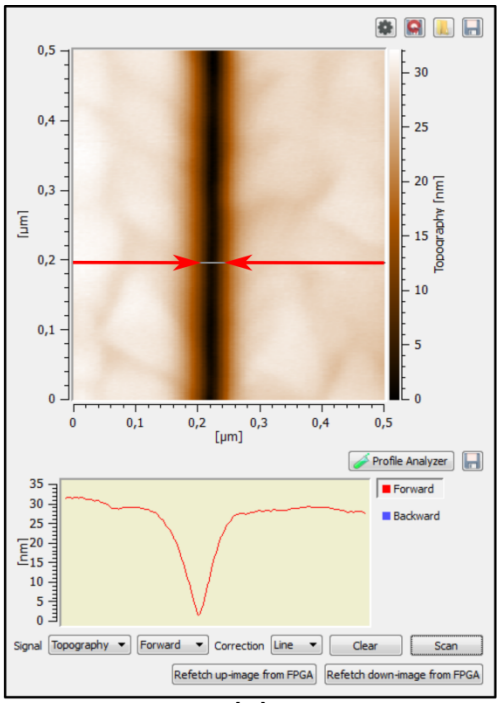

(a)

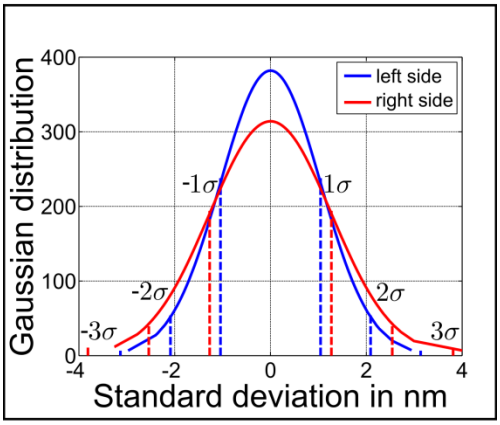

(b)

Fig. 11.9.4 Reproducibility test. (a): Line scan topography profile obtained 200 times during trench scan. (b): The detected deviation values for trench edges are within ±3-4 nm (3σ).

The carried out proof of concept consists of positioning of the sample with respect to the mini-AFMs, followed by analysis of the positioning error, which is related to the specifications of the wafer carrying bottom stage. The setup allows an optical navigation towards the alignment mark position. After that, the mini-AFMs analyze the marks and the control-unit (together with the software module) is used to

calculate all offsets, in particular Δx, Δy, and rotation $\Delta\varphi$. In a next step the offsets are transmitted to the high precision mechanical alignment x, y, φ motors (the x, y - scanning orthogonality of the mini-AFMs are precisely specified by using a high precision metrology tool (Nanopositioning and Nanomeasuring Machine from SIOS GmbH, Ilmenau) [11].

In our PoC system the bottom positioning stage is used for steering of the sample in order to compensate the detected offset errors. The alignment accuracy of the presented system depends on the movement steps of the stage. The currently used bottom positioning stage has a movement resolution of 10 nm.

Employing the currently available bottom positioning stage a statistics of the bottom stage positioning accuracy was measured, summarized in Fig. 11.9.5.

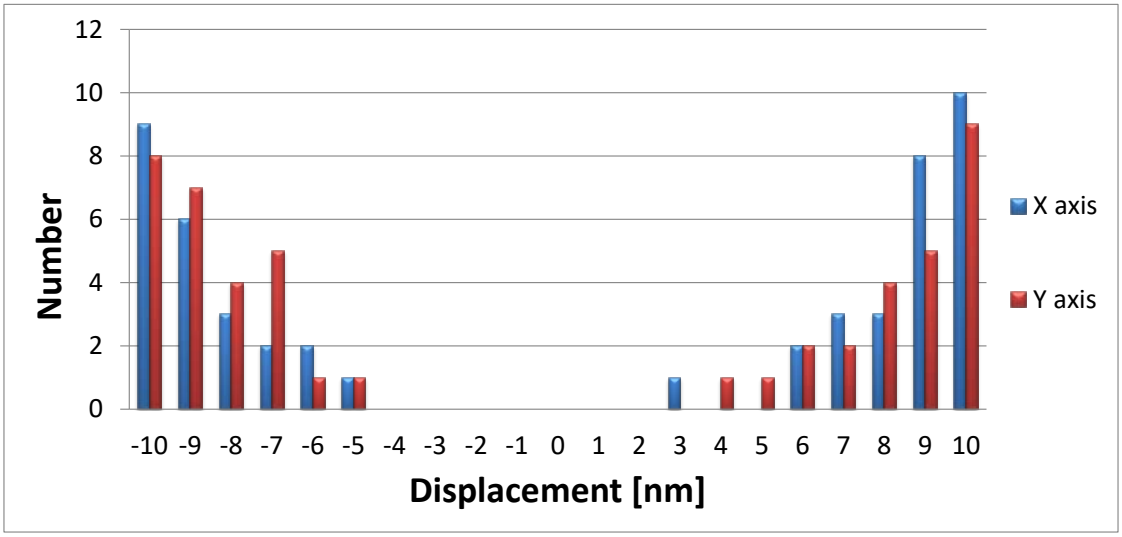

Fig. 11.9.5 Statistics for the measured bottom stage positioning accuracy with respect to the alignment mark center. Total number of the repeated trials is 50.

In terms of this process, a target alignment mark was selected on the wafer and the positioning procedure was repeated 50-times on the same mark. Every positioning process included the following steps, which are executed sequentially: i) The mini-AFM is placed over another alignment mark (different from the selected target mark) by moving the wafer with the bottom positioning stage; ii) The mini-AFM is placed over the target alignment mark by driving the stage back to the measured

coordinates of the selected mark; iii) The system measures the offset between the alignment mark center and the position of the mini-AFM emulating the lithographic template (the used measurement procedure employing a cross-correlation technique was described in detail in the deliverable report D11.6), and; iv) The detected offset is compensated by calculated bottom stage movements. For the compensation movement, an additional condition is imposed defining that the stage position error (the difference between the commanded position and the actual position) should be less than a predefined threshold value. This is achieved by using the closed loop control system of the stage taking into account the internally calculated position error. In order to address a sub-10 nm positioning accuracy of the bottom stage we used a threshold value of 10 nm. As a result, we obtained the deviation statistics summarized in Fig. 11.9.5. In general, the total measurement error for the developed alignment method includes:

- Line edge roughness (LER) of the alignment features,
- The thermal drift of the top-frame with respect to the two mini-AFM systems,
- The accuracy of the pre-patterned alignment mark position,
- The measurement accuracy of the position of the mini-AFM tips,
- The surface roughness of the spin-coated resist layer,
- Total electronic noise associated with the AFM imaging process.

- **Summary**

With this report, we intend to present a general setup for statistical evaluation of the considered overlay alignment technique.

Within the test series carried out the developed PoC system was employed for accurate positioning of the processed semiconductor wafer. During emulation of the developed alignment method the offset between the alignment mark patterns on the wafer and the mini-AFMs was measured. The obtained AFM images are used to

	calculate the deviation and steer the bottom stage carrying the wafer in order to achieve the desired offset accuracy. The detection of the offset error is carried out by using "X"-shaped marks, measured by integrated mini-AFM units. In this manner the three degrees of freedom are measured: x, y and φ (rotation around z-axis), wherein a cross-correlation method was used to determine the relevant position parameters. The obtained results successfully demonstrate the proof of concept of the considered scanning probe based alignment method. Statistical data was gathered for positioning of the bottom stage carrying the processed wafer sample, whereas the positioning procedure was performed 50 times onto a preliminary selected alignment mark. Due to the obtained statistical data regarding the positioning error, at the moment, PoC setup is able to determine the positioning error of the bottom stage carrying the processed wafer sample with an accuracy of below 10 nm (8.8 nm rms). This result was obtained without temperature compensation. The demonstrated proof of concept is theoretically being able to deliver sub-5 nm resolution. However, to achieve this target additional engineering work and financial efforts are required. In order to improve the realized proof of concept system a precise thermal stabilization should be considered involving also the utilization of materials with low expansion coefficients. In this case, taking into account the superior scan resolution the AFM systems are capable of, the accuracy of the actual test setup could be significantly improved reaching possibly the sub-nanometer accuracy.
Explanation of Differences between Estimation and Realization	It is required that the mini-AFMs have to be integrated onto template made from quartz. Since the fabrication of a real tool (schematically shown in Fig. 11.9.1) is highly expensive, it was decided as a first step, to build a proof of concept (PoC) setup (shown in Fig. 11.9.2) in order to test the developed overlay alignment method. Herein, the overlay alignment procedure is emulated. The emulation considers a virtual template connected to the two mini-AFM heads. The obtained

AFM images of alignment marks are used for detection of the offset between the processed wafer sample and the two mini-AFMs. Obviously, we assume a correct calibration of the template with respect to the mini-AFM heads. Using such an approach, where the entire template is not integrated into the system and only virtual template (represented by two mini-AFMs) is considered, an overlay between different lithographic patterns was not realized. Thus, at the current stage of development it is not possible to conclude on a real imprint alignment process. However, the POC setup is used for evaluation of the most crucial point, the positioning of the bottom stage carrying the processed wafer with high accuracy preferably better than 10 nm by applying the developed method and routines. With respect to reliability, it is necessity to create a framework that identifies and corrects sources of artifacts and provides real-time fidelity measures on inferences from measurements in mini-AFMs.

To get realistic answer with respect to the reliability of the mini-AFMs, we have recorded 50 images (see Fig. 11.9.5), which should represent the real surface structure. We consider that we are in real non-contact mode and the tip remains unchanged. We used forward and backward scanning directions and studied the shift of the images (for homogeneous lithographic features). Additionally, we studied the tip shape influence and the tip-surface forces at different interaction conditions due to setting the damping of the oscillating cantilever.

In the best case, sub-5nm tip interacts with the surface to obtain profile of the SPL features with size smaller than 10 nm. However, the structure, shape, and surface hardness of the used tips are usually poorly defined or even unknown. We used SEM to examine the changes in the tip after the AFM imaging, and analyzed the surface contamination. Another source influencing the reliability of the AFM measurements was the drift occurring during the experiments. Ideally, high-speed imaging is another option to reduce the drift. The realization of high-speed mini-AFMs, operating in either static or dynamic modes, requires significant enhancements in the hardware and software, and reduction of the size of the cantilevers, which

	results in high resonant frequency. Additionally, the use of piezoresistive self-actuated cantilever requires electronics with high feedback bandwidth, high-speed scanners, and high- speed data-acquisition system. After introducing of some improvements into the mini-AFMs the scanning speed was increased to 20 lines per second. In this manner, we got measurable reduction of the drift. In terms of the durability issues, we studied mainly the lifetime of the AFM tips. We found out that the measurement regime is deciding factor for long-time stable operation of the mini-AFMs. The AFM based on previously mentioned cantilever techniques allows precise judgement of the operation modes by the choice of the set point. The favorable mode is real “non-contact mode” which however is often noisy and surface sensitive. We decided to apply mode between non-contact and tapping mode which is somehow a compromise with respect to the durability of the tip.
Metrology comments	For the current PoC system a measurement deviation of ±3-4 nm 3σ has been measured. The deviation can be reduced by downsizing the pixel size (from 1.9 nm to 0.5 nm), which is achievable either by enhancement of the scan resolution, e.g. 1024 pixel/line, or by reduction of the scan area. Herein, the actual measurement in Fig. 11.9.4 was limited since computational efforts should be minimized. Additionally, taking into account the measurement time and the absence of a thermal stabilization, the measured deviation can be explained. Thus, we suppose that in case of employing the system under cleanroom conditions the deviation value should be further reduced. The x,y - scanning orthogonality of the mini-AFMs are precisely specified by using a high precision metrology tool (Nanopositioning and Nanomeasuring Machine from SIOS GmbH, Ilmenau) [11]. The mini-AFM systems were calibrated in z-direction using HOPG samples. We used as calibration standard others samples previously calibrated at VSL. The metrology chips made by IMEC were verified by VSL and used for calibration of the commercial

	microscopes (ASYLUM and BRUKER) installed at TUIL.
References	[1] M. Neisser, S. Wurm, Adv. Opt. Techn. 4(4): 235–240 (2015) [2] http://www.itrs.net/ITRS 201999-2014 Mtgs, Presentations & Links/2011ITRS/2011Chapters/2011Lithography.pdf [3] http://ieuvi.org/TWG/Mask/2013/MTG022413/13__ITRS_Roadmapping_Process__Frank_Goodwin [4] T. Higashiki, T. Nakasugi, I. Yoneda, J. Micro/Nanolith. MEMS MOEMS 10(4), 043008 (2011) [5] C. Peroz, S. Dhuey, M. Volger, Y. Wu, D. Olynick, S. Cabrini, Nanotechnology 21, 445301 (2010) [6] I. W. Rangelow, European patent No. EP 1 617 293 A1 (18 January 2006) [7] V. Ishchuk, E. Guliyev, C. Aydogan, I. Buliev, M. Kaestner, Tzv. Ivanov, A. Ahmad, A. Reum, S. Lenk, C. Lenk, N. Nikolov, Th. Glinsner, I.W. Rangelow, Applied Physics A, 123(1), 1–12 (2017). [8] E. Guliyev, Th. Michels, B.E. Volland, Tzv. Ivanov, M. Hofer, I.W. Rangelow, Microelectron. Eng. 98, 520–523 (2012) [9] C. Rawlings, U. Duerig, J. Hedrick, A.W. Knoll, IEEE Transactions on Nanotechnology 13(6) (2014) [10] V. Ishchuk, D.L. Olynick, Z. Liu, I.W. Rangelow, J. Appl. Phys. 118, 053302 (2015) [11] N. Vorbringer-Doroshovets, F. Balzer, R. Fuessl, E. Manske, M. Kaestner, A. Schuh, J.-P. Zoellner, M. Hofer, E. Guliyev, A. Ahmad, T. Ivanov, I. W. Rangelow., Proc. SPIE 8680, 868018 (2013)